Ultrathin Gold Island Films on Silanized Glass. Morphology and Optical Properties

Ilanit Doron-Mor,[†] Zahava Barkay,[‡] Neta Filip-Granit,[†] Alexander Vaskevich,[†] and Israel Rubinstein*,[†]

Department of Materials and Interfaces, Weizmann Institute of Science, Rehovot 76100, Israel, and Wolfson Materials center, Tel-Aviv University, Tel-Aviv 69978, Israel

Received March 9, 2004. Revised Manuscript Received June 18, 2004

Evaporated gold island films have been the subject of studies dealing with a variety of spectroscopic and sensing applications. Development of these and other applications requires film stability as well as tunability of the morphology and optical properties of the island films. In the present work, ultrathin, island-type gold films were prepared by evaporation of 1.0−15.0 nm (nominal thickness) gold at a rate of 0.005−0.012 nm s^{-1} onto glass substrates modified with 3-mercaptopropyl trimethoxysilane (MPTS), the latter used to improve the Au adhesion to the glass. The morphology of the films, either unannealed or annealed (20 h at 200 °C), was studied using atomic force microscopy (AFM) and high-resolution scanning electron microscopy (HR-SEM). The information provided by the two imaging techniques is complementary, giving a good estimate of the shape of the islands and its variation with film thickness and annealing. The optical properties of the films were examined using transmission UV−vis spectroscopy, showing a strong dependence of the localized Au surface plasmon (SP) band on the morphology of the island films. The imaging and spectroscopy indicate a gradual transition from isolated islands to a continuous film upon increasing the Au thickness.

Introduction

Discontinuous evaporated gold films have been used in various applications, including sensing based on transmission surface plasmon resonance (T-SPR) spectroscopy,[1−3] surface-enhanced Raman spectroscopy (SERS),[4−10] and infrared spectroscopy.[11−16] The morphology of such films has been studied previously.[17] Ultrathin (ca., 1−10 nm) island-type films of noble metals (Au, Ag, Cu) evaporated on transparent substrates exhibit transmission spectra showing an absorption band attributed to localized surface plasmon (SP) excitation, similar to systems consisting of dispersed metal particles.[18] The localized SP absorption characteristic of such films is highly sensitive to the dielectric constant of the surrounding medium;[19−22] hence, changes in the immediate environment of the island surface can be monitored by changes in the SP absorption band, using transmission UV−vis spectroscopy. The optical response is sensitive enough to monitor adsorption of molecules on the metal island surface down to (sub)-monolayer coverage,[1,23] follow changes in the chain length of alkanethiol self-assembled monolayers,[24] or follow changes in the concentration of analytes in solution.[25] The method was termed transmission surface plasmon resonance (T-SPR) spectroscopy, and its use-

* To whom correspondence should be addressed. Telephone: 972-8-9342678. Fax: 972-8-9344137. E-mail: israel.rubinstein@weizmann.ac.il.
[†] Weizmann Institute of Science.
[‡] Tel-Aviv University.

(1) Kalyuzhny, G.; Schneeweiss, M. A.; Shanzer, A.; Vaskevich, A.; Rubinstein, I. *J. Am. Chem. Soc.* **2001**, *123*, 3177−3178.
(2) Kalyuzhny, G.; Vaskevich, A.; Schneeweiss, M. A.; Rubinstein, I. *Chem.-Eur. J.* **2002**, *8*, 3850−3857.
(3) Lahav, M.; Vaskevich, A.; Rubinstein, I., *Langmuir*, **2004**, *20*, 7365−7367.
(4) Sockalingum, G. D.; Beljebbar, A.; Morjani, H.; Angiboust, J. F.; Manfait, M. *Biospectroscopy* **1998**, *4*, S71−S78.
(5) Mosier-Boss, P. A.; Lieberman, S. H. *Appl. Spectrosc.* **1999**, *53*, 862−873.
(6) Ye, Q.; Fang, J. X.; Sun, L. *J. Phys. Chem. B* **1997**, *101*, 8221−8224.
(7) Tsen, M.; Sun, L. *Anal. Chim. Acta* **1995**, *307*, 333−340.
(8) Gupta, R.; Dyer, M. J.; Weimer, W. A. *J. Appl. Phys.* **2002**, *92*, 5264−5271.
(9) Gupta, R.; Weimer, W. A. *Chem. Phys. Lett.* **2003**, *374*, 302−306.
(10) Jensen, T.; Kelly, L.; Lazarides, A.; Schatz, G. C. *J. Cluster Sci.* **1999**, *10*, 295−317.
(11) Goutev, N.; Futamata, M. *Appl. Spectrosc.* **2003**, *57*, 506−513.
(12) Niklasson, G. A.; Granqvist, C. G. *Appl. Phys. Lett.* **1985**, *46*, 713−715.
(13) Osawa, M.; Ataka, K.; Yoshii, K.; Nishikawa, Y. *Appl. Spectrosc.* **1993**, *47*, 1497−1502.
(14) Smith, G. B. *Appl. Phys. Lett.* **1985**, *46*, 716−718.
(15) Smith, G. B.; Niklasson, G. A.; Svensson, J.; Granqvist, C. G. *Sol. Energy Mater.* **1986**, *14*, 257−268.
(16) Smith, G. B.; Niklasson, G. A.; Svensson, J.; Granqvist, C. G. *J. Appl. Phys.* **1986**, *59*, 571−581.
(17) Andersson, T. *Thin Solid Films* **1975**, *29*, L21−L23.
(18) Kreibig, U.; Bour, G.; Hilger, A.; Gartz, M. *Phys. Status Solidi* **1999**, *175*, 351−366.
(19) Papavassiliou, G. C. *Z. Phys. Chem.-Leipzig* **1976**, *257*, 241−248.
(20) Orfanides, P.; Buckner, T. F.; Buncick, M. C.; Meriaudeau, F.; Ferrell, T. L. *Am. J. Phys.* **2000**, *68*, 936−942.
(21) Mock, J. J.; Smith, D. R.; Schultz, S. *Nano Lett.* **2003**, *3*, 485−491.
(22) Jensen, T. R.; Duval, M. L.; Kelly, K. L.; Lazarides, A. A.; Schatz, G. C.; Van Duyne, R. P. *J. Phys. Chem. B* **1999**, *103*, 9846−9853.
(23) Kalyuzhny, G.; Vaskevich, A.; Ashkenasy, G.; Shanzer, A.; Rubinstein, I. *J. Phys. Chem. B* **2000**, *104*, 8238−8244.
(24) Malinsky, M. D.; Kelly, K. L.; Schatz, G. C.; Van Duyne, R. P. *J. Am. Chem. Soc.* **2001**, *123*, 1471−1482.
(25) Gluodenis, M.; Manley, C.; Foss, C. A. *Anal. Chem.* **1999**, *71*, 4554−4558.

10.1021/cm049605a CCC: $27.50
Published on Web 08/14/2004

fulness in various sensing applications, in the gas or liquid phase, was demonstrated.[2] Biological applications of T-SPR spectroscopy in detecting DNA hybridization[26] and in specific protein recognition[3] appear promising for biosensing.

Ag and Au island films have been widely used in surface-enhanced Raman spectroscopy (SERS) and infrared spectroscopy, based on the local increase of the electromagnetic field near the surface of metal islands.[13,27] Despite extensive efforts during more than two decades, reliable platforms for high-sensitivity output in both methods are still being sought, with emphasis on optimization of the film morphology.[4,8,9,28]

In the present work, glass slides served as substrates for Au evaporation, offering a smooth, transparent, chemically inert, and inexpensive platform, yet known to exhibit poor adhesion to noble metals. Hence, Au island films evaporated on bare glass show poor stability in various solvents, including water.[5] A similar problem was encountered with Ag island films on glass.[29] Improvement of the adhesion is commonly achieved by evaporation of a 5−10 nm Cr, Ni, or Ti underlayer.[30] However, strong damping of the SERS signal was found for Au island films evaporated on a metal underlayer,[5] and the absorbance of the metal (oxide) adhesion layer would impose additional requirements on the optical instrumentation. A viable possibility for improvement of evaporated metal adhesion is precoating the glass substrate with a self-assembled layer of a mercapto- or amino-silane.[5,31−33] The glass substrates used in the present work were therefore pretreated with 3-mercaptopropyl trimethoxysilane (MPTS) to improve the adhesion of the Au to the glass.[31]

The morphology and optical properties of Au island films on several substrates have been studied previously. The structure and absorbance of Au island films evaporated on bare mica and quartz were reported[1,2,23] in the context of the development of T-SPR spectroscopy. However, Au island films grown on an adhesive substrate, that is, on glass precoated with a silane adhesion layer as reported here, have not been studied.

While the optical response of ultrathin, semi-transparent Au island films can be conveniently measured using transmission spectroscopy, a detailed study of the morphology requires high-resolution imaging techniques. Transmission electron microscopy (TEM), commonly used for characterization of film structure down to atomic resolution, provides a quantitative description of the 2D projection of the island ensemble,[34−37] but involves highly complex sample preparation due to the difficulty in separating the island film from the substrate while leaving the film intact. A better choice is scanning electron microscopy (SEM) imaging, which requires no particular sample preparation and allows imaging of Au island films with a resolution of several nanometers, as demonstrated with silicon[8] and titania[38] substrates. In the present work, application of high-resolution SEM (HR-SEM) enables imaging of Au island films on insulating glass substrate at a high resolution. The two-dimensional images obtained by HR-SEM are complemented here by the three-dimensional atomic force microscopy (AFM) imaging, the latter providing sub-nanometer sensitivity in the perpendicular direction. The combination of the two imaging techniques provides information on the shape of the Au islands as well as insight into the mechanism of film growth.

The relationship between the morphology and optical properties of such films has direct bearing on the sensitivity and optimization of T-SPR measurements and is the subject of the present work.

Experimental Section

Chemicals. Chloroform (Biolab, AR) was passed through a column of activated basic alumina. Ethanol (Merck, AR), 2-propanol (Frutarom, Israel), H_2O_2 (30%, Frutarom, Israel), H_2SO_4 (95−98%, Palacid, Israel), and 3-mercaptopropyl trimethoxysilane (MPTS) (97%, Aldrich) were used as received. Water was triply distilled. The gas used was purified house nitrogen (from liquid N_2).

Gold Film Preparation. Glass slides (10 × 18 mm^2) No. 2 (Menzel-Glaser, Germany) were immersed in freshly prepared "piranha" solution (1:3 H_2O_2 30%:H_2SO_4 95−98%) for 15 min and rinsed with triply distilled water. (*Caution: Piranha solution reacts violently with organic materials and should be handled with extreme care.*) This procedure was repeated twice, after which the slides were rinsed with ethanol, dried under a nitrogen stream, and held for ca. 10 min at 100 °C. The slides were immersed for 10 min in a mixture of 1.9 mL of MPTS, 1.4 mL of water, and 100 mL of 2-propanol, which was brought to reflux, then rinsed with 2-propanol, dried under a nitrogen stream, and cured in an oven at 100−107 °C for 8 min. The silanization procedure was carried out three times.[31] The silanized glass slides were mounted in a cryo-HV evaporator (Key High Vacuum) equipped with a Maxtek TM-100 thickness monitor for evaporation of the ultrathin Au films. Homogeneous Au deposition was achieved by moderate rotation of the substrate plate. Gold (99.99%, Holland-Moran, Israel) was evaporated from a tungsten boat at (2−4) × 10^{-6} Torr, at a deposition rate of 0.005−0.012 nm s^{-1}. The temperature in the evaporation chamber, monitored using a thermocouple located near the substrate plate, rises with film thickness from ca. 50 °C for 1.0 nm films to ca. 100 °C for 15 nm films. Details on the evaporation parameters are given as Supporting Information.

Postdeposition annealing of Au-covered slides was carried out in air at 200 °C for 20 h, using a Ney Vulcan 3-550 oven. The heating rate was 5 °C min^{-1}, and the annealed slides were left to cool in air to room temperature.

UV−Vis Spectroscopy. Measurements were carried out ex situ (in air) using a Varian CARY 50 UV/VIS/NIR spectrophotometer with a specially designed holder.[2] The scan rate was 600 nm min^{-1}, and the bandwidth of the light source in the UV−vis region was 1.0 nm. A baseline correction procedure

(26) Hutter, E.; Pileni, M. P. *J. Phys. Chem. B* **2003**, *107*, 6497−6499.
(27) Gersten, J.; Nitzan, A. *J. Chem. Phys.* **1980**, *73*, 3023−3037.
(28) Jensen, T. R.; Van Duyne, R. P.; Johnson, S. A.; Maroni, V. A. *Appl. Spectrosc.* **2000**, *54*, 371−377.
(29) Riboh, J. C.; Haes, A. J.; McFarland, A. D.; Yonzon, C. R.; Van Duyne, R. P. *J. Phys. Chem. B* **2003**, *107*, 1772−1780.
(30) Schneeweiss, M. A.; Rubinstein, I. In *Encyclopedia of Electrochemistry Vol. 10*; Bard, A. J., Stratmann, M. (Eds.), Fujihira, M., Rubinstein, I. (Volume Eds.); Wiley-VCH, submitted for publication.
(31) Goss, C. A.; Charych, D. H.; Majda, M. *Anal. Chem.* **1991**, *63*, 85−88.
(32) Malynych, S. Z.; Chumanov, G. *J. Vac. Sci. Technol., A* **2003**, *21*, 723−727.
(33) Wanunu, M.; Vaskevich, A.; Rubinstein, I. *J. Am. Chem. Soc.* **2004**, *126*, 5569−5576.
(34) Doremus, R. *Thin Solid Films* **1998**, *326*, 205−210.
(35) Norrman, S. H.; Andersson, T. G. *Thin Solid Films* **1980**, *69*, 327−337.
(36) Norrman, S.; Kulyupin, Y.; Andersson, T. *Thin Solid Films* **1980**, *67*, L49−L51.
(37) Norrman, S.; Andersson, T.; Peto, G.; Somogyi, S. *Thin Solid Films* **1981**, *77*, 359−366.
(38) Zhang, L.; Cosandey, F.; Persaud, R.; Madey, T. E. *Surf. Sci.* **1999**, *439*, 73−85.

(the spectrum of air was taken as baseline) was executed prior to each measurement session.

Atomic Force Microscopy (AFM). AFM images were recorded in air using a Molecular Imaging PicoScan (Pico IC) instrument operated in the acoustic AC (AAC) mode. The cantilevers used were NSC12 series of ultrasharp silicon (MikroMash, Estonia), with a resonant frequency of 100−200 kHz and an average tip radius of ≤10 nm.

High-Resolution Scanning Electron Microscopy (HR-SEM). Images were obtained using a JSM-6700F high-resolution scanning electron microscope with a cold field emission electron source and upper built-in SE detector. Low-energy SE signal suppression was performed to reduce the charging effect in the SE images, particularly important for the 1.0 and 2.5 nm samples. Statistical analysis of HR-SEM images was carried out using an image processing software (ImageJ 1.29x, Wayne Rasband, National Institute of Health, USA; http://rsb.info.nih.gov/ij).

Results and Discussion

Preparation and Stabilization of Au Island Films. Ultrathin Au island films with nominal thicknesses of 1.0, 2.5, 5.0, 7.5, 10.0, and 15.0 nm were evaporated on MPTS-modified glass substrates at an evaporation rate of 0.005−0.012 nm s^{-1}. The excellent adhesion provided by MPTS interlayers to Au films evaporated on glass is well established.[5,31] Annealing has been used for tuning the optical properties (intensity and wavelength of the localized SP band) and morphology of Au island films.[1,2,23,39] Here, the samples were annealed in air at 200 °C for 20 h. The relatively low temperature and long annealing time (we previously used 250 °C for 3−4 h for annealing of films on bare substrates[2,23]) were chosen to protect the organic adhesive layer (low temperature) while enabling Au island reorganization (long time). Hence, 2.5 nm Au island films, both unannealed and annealed, passed successfully the adhesive tape test[31] (Scotch, Magic transparent), demonstrating the good adhesion provided by the MPTS interlayer and its stability under the annealing conditions. A transmission UV−vis spectrum was recorded for each substrate after Au deposition, and samples that showed substantial deviation from the average spectrum were discarded (about 15% of the samples).

All of the samples were stabilized by dipping in 1:1 $CHCl_3$/EtOH (solvents commonly used for self-assembly of organic mono-/multilayers[40,41]) and drying under a stream of nitrogen. The indication for stability of the Au island films was the SP extinction peak measured in air, which stopped changing after about 10 min in the solution (this time varied somewhat between samples). Figure 1 demonstrates the effect of the solvent on the optical properties of 2.5 nm films. The immersion induces a small blue shift of the optical spectrum and a marked decrease in the optical density; the same trend is observed for the other thicknesses, as well as with other solvents, for example, water (not shown). These spectral changes are attributed to the effect of wetting and drying on the fine morphology of the Au islands,

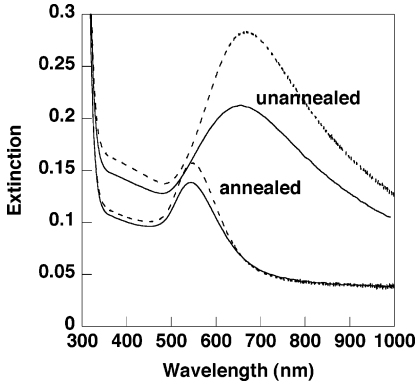

Figure 1. UV−vis spectra of 2.5 nm gold films on silanized glass (measured ex situ), immediately after evaporation or annealing (dashed lines) and after dipping in 1:1 $CHCl_3$/EtOH solution until stabilization of the SP absorption band was observed (solid lines).

an effect known for Ag island films,[24,42−44] directly influencing the Au surface plasmon absorbance.

Morphology of Au Island Films. Figure 2 shows HR-SEM and AFM images of the Au films (1.0−15.0 nm nominal thickness). In general, the average island size increases with thickness; a situation close to percolation is seen at about 15.0 nm for the unannealed film, in agreement with the optical results discussed below. The percolation threshold is sensitive to the film thickness, the evaporation rate, and the annealing process. The effect of the evaporation rate is particularly intriguing; hence, evaporation of 15.0 nm Au on similar substrates at faster rates (0.05−0.1 nm s^{-1}) produces continuous films on both annealed and unannealed samples,[33] while at the lower rates used here an island morphology is obtained. Under the present conditions, annealing leads to an increase in the average area of individual islands and of the average distance between islands, as well as to a change in the island shape. These changes are quite similar to those observed with other substrates,[2,23] suggesting that island mobility and coalescence is the predominant mechanism responsible for the morphology change induced by annealing. Note that temperature rise during evaporation, induced by the heated evaporation source (see Supporting Information), may have an influence on the island morphology. This factor varies for different evaporators and should be taken into consideration.

HR-SEM and AFM studies of 2.5 nm Au films before and after solvent stabilization (see above) did not reveal any visible change in the island organization or morphology. This suggests that the mechanism responsible for the marked change in the optical spectra upon immersion and drying (Figure 1) involves structural changes that are not visible in the 2D projection of the HR-SEM or in the AFM topography of the islands, for example, possible alteration of the shape at the island/substrate interface. This intriguing effect requires further study.

Statistical analysis of the HR-SEM images was carried out using ImageJ image processing software. The

(39) Meriaudeau, F.; Wig, A.; Passian, A.; Downey, T.; Buncick, M.; Ferrell, T. L. *Sens. Actuators, B* **2000**, *69*, 51−57.
(40) Hatzor, A.; Moav, T.; Cohen, H.; Matlis, S.; Libman, J.; Vaskevich, A.; Shanzer, A.; Rubinstein, I. *J. Am. Chem. Soc.* **1998**, *120*, 13469−13477.
(41) Doron-Mor, I.; Hatzor, A.; Vaskevich, A.; van der Boom-Moavt, T.; Shanzer, A.; Rubinstein, I.; Cohen, H. *Nature* **2000**, *406*, 382−385.
(42) Roark, S. E.; Semin, D. J.; Lo, A.; Skodje, R. T.; Rowlen, K. L. *Anal. Chim. Acta* **1995**, *307*, 341−353.
(43) Roark, S. E.; Rowlen, K. L. *Anal. Chem.* **1994**, *66*, 261−270.
(44) Roark, S. E.; Semin, D. J.; Rowlen, K. L. *Anal. Chem.* **1996**, *68*, 473−480.

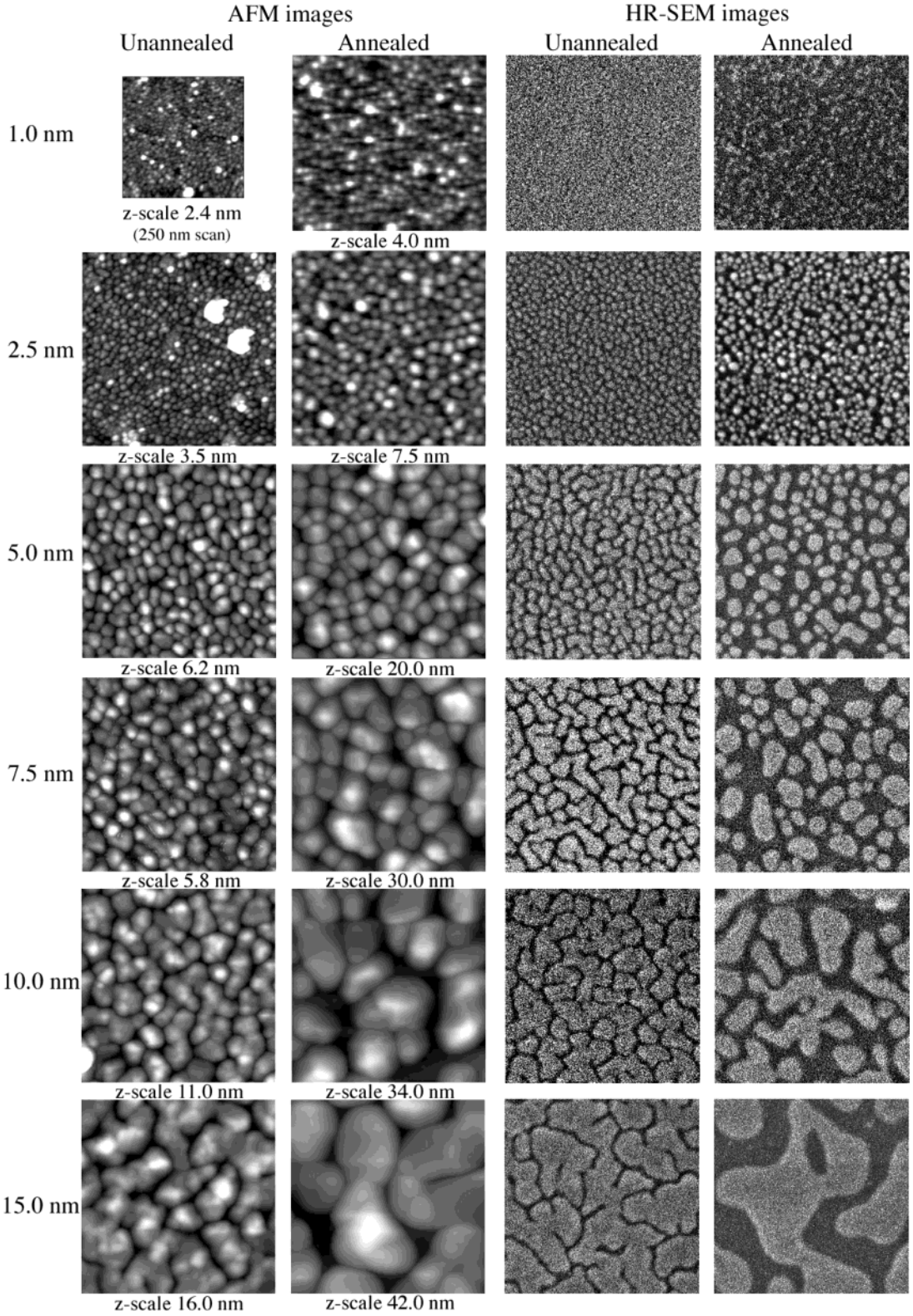

Figure 2. AAC mode AFM and HR-SEM images (400 × 400 nm^2) of ultrathin gold island films on silanized glass. Nominal thickness (left), *z*-scale (under each AFM image), and preparation conditions (top) are indicated.

procedure included threshold image intensity adjustment that enabled the software to identify the islands, thus providing a good estimate of the Au coverage. In the 1.0 nm unannealed sample, the islands were inseparable by the software, and this sample was therefore not included in the analysis. The overall area fraction of the Au islands was produced by analysis of the Au coverage (Figure 3). In general, the area fraction of unannealed Au island films is larger and grows faster with thickness than that of the corresponding annealed films. This reflects the effect of annealing, that is, joining adjacent islands while increasing the average island height as well as the average separation between islands.

The average island area was also extracted using the image processing software. The average separation

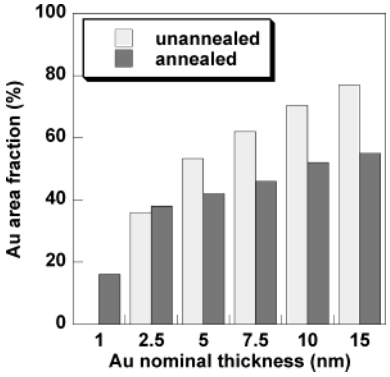

Figure 3. Fractional coverage of the glass by Au islands versus Au nominal thickness. Data were obtained by image processing (ImageJ software) of HR-SEM images.

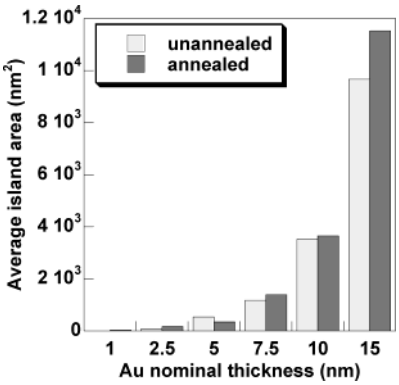

Figure 4. Average area of individual Au islands versus Au nominal thickness. Data were obtained by image processing (ImageJ software) of HR-SEM images.

between islands, not obtainable by the image processing procedure, was derived manually by superposing a grid on each image and measuring the separation between islands along all of the lines in the grid, and averaging. This procedure is rather inaccurate for the 1.0 and 2.5 nm films due to the small interisland separation, as seen in Figure 2. For the 2.5 nm samples, an array of circular-shaped islands was assumed, and the average separation between islands was estimated from the overall area fraction and the average island size. For the 1.0 nm annealed films, these assumptions cannot be used due to the formation of "chains" of islands; hence, the 1.0 nm films were not included in the analysis.

The results are shown in Figures 4 and 5. For the unannealed films, the average island area (Figure 4) grows substantially as the gold thickness increases, while the average separation between the islands (Figure 5) increases moderately. Intuitively, the separation between islands in the unannealed films should not increase, or even decrease, as more material is added. The results therefore suggest that Au island coalescence and reshaping proceeds during Au evaporation on the time scale of minutes, influencing the morphology of unannealed films. This process is enhanced by secondary annealing during evaporation (induced by the heated source), more pronounced for longer evaporations (higher thicknesses) (see Supporting Information). In the annealed films, the average island area (Figure 4) and the average separation between the islands (Figure 5) grow substantially as the Au thickness increases,

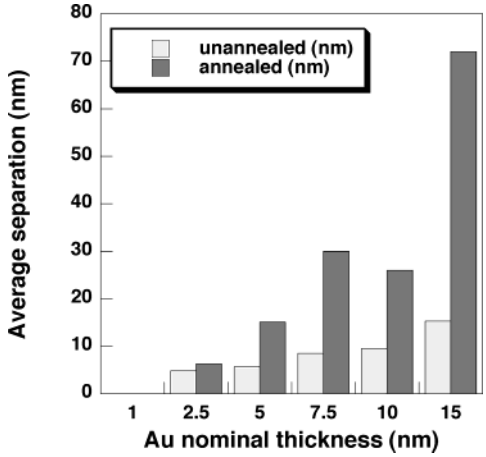

Figure 5. Average separation between islands versus Au nominal thickness. Data were obtained by statistical analysis of HR-SEM images.

implying a marked increase in island height of the annealed films.

Information on the Au island height (*z*-scale information) can be obtained by AFM imaging. Figure 2 shows AAC mode AFM images of Au films similar to those analyzed by HR-SEM. The Au islands appear larger in diameter, more rounded, and closer to each other in the AFM images as compared to the corresponding HR-SEM images, resulting from AFM tip convolution. Hence, the lateral island dimensions in the AFM images are not reliable, yet AFM provides viable information on the island height, not available in the 2D HR-SEM imaging. The data provided by the two techniques are complementary and, when combined, can give valuable estimates of the island shape.

To address the AFM tip convolution issue in the present case, the total number of Au islands, counted directly from the HR-SEM and AFM images of unannealed films (Figure 2), were compared for different nominal thicknesses (Table 1). As expected, the Au island density in the HR-SEM images is higher than that in the corresponding AFM images. The difference in island density (Table 1) decreases from 12% (2.5 nm films) to 7% (5.0 nm films) and is close to zero for 7.5 nm film and above. Combining these data with the measured average separation between islands (Figure 5) indicates an approximate lateral limit of ca. 10 nm for true island separation in our AFM imaging, in agreement with the tip radius (≤10 nm according to specifications).

The AFM results are presented in Figure 6 as the average island height (obtained by statistical analysis of the AFM images in Figure 2) versus Au nominal thickness. Also plotted in Figure 6 are (i) the theoretical thickness of a homogeneous, continuous film grown to the nominal thickness, that is, a straight line with a 45° slope; and (ii) average island height calculated from the area fraction data (Figure 3) (nominal thickness/area fraction) for the unannealed and annealed films. As seen in Figure 6, the AFM measured average height of the unannealed films is lower than the thickness calculated from the area fraction, and lower even than the nominal thickness. This again is a manifestation of substantial tip convolution, as the largest average separation between islands for unannealed films is ca.

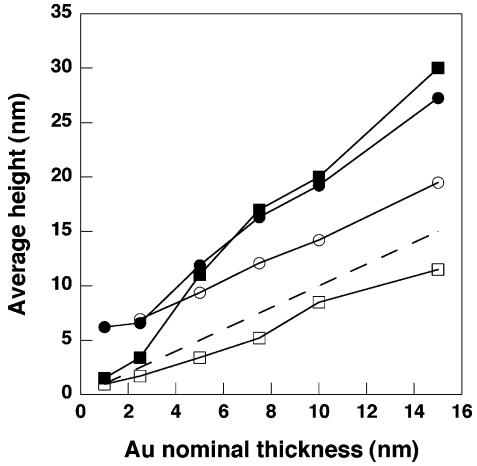

Figure 6. Average height of Au islands versus Au nominal thickness, showing data obtained by statistical analysis of AFM images (squares); data calculated from the Au area fraction (circles); and nominal thickness (dashed line). Open and full symbols represent unannealed and annealed samples, respectively. Lines through the experimental points are drawn as guides to the eye.

Table 1. Island Density in Unannealed Au Island Films on Silanized Glass

Au film nominal thickness, nm	Au island density, μm^{-2}		
	AFM image	HR-SEM image	% difference
2.5	1760	2000	12
5.0	676	728	7
7.5	284	292	3

15 nm (for the 15 nm film, see Figure 5). For annealed films, the average AFM measured height is lower than that calculated from the area fraction for films below 5.0 nm (nominal thickness) (Figure 6), which is the thickness where the separation between islands is also ca. 15.0 nm (Figure 5). Above 5.0 nm (nominal thickness), the AFM measured island height of annealed films follows fairly closely the height calculated from the area fraction, giving somewhat larger values (probably associated with the island shape) and indicating little, if any, tip convolution for these samples.

Evolution of the Au island film morphology with increasing thickness, as was observed in this study, raises the issue of high total island area at percolation (about 80% surface coverage for unannealed films near percolation, see Figure 3).[45] This indicates the major impact of island mobility, coalescence, and reshaping during evaporation on the film morphology. The rather small difference of 12% in island density observed in AFM versus HR-SEM images of 2.5 nm films (even smaller for larger thicknesses) (Table 1) suggests that the 2-D shape of the islands seen in the AFM images is generally correct, as was also revealed by comparison with HR-SEM images (Figure 2). A magnified image of a 2.5 nm unannealed film shows round-shaped islands (Figure 7a), which can be described as oblate ellipsoids.[46] The shape of contacting islands is close to that of individual ones, indicating a small degree of island coalescence. AFM images of the 5.0 and 7.5 nm films show considerably more interconnected chains (Figure

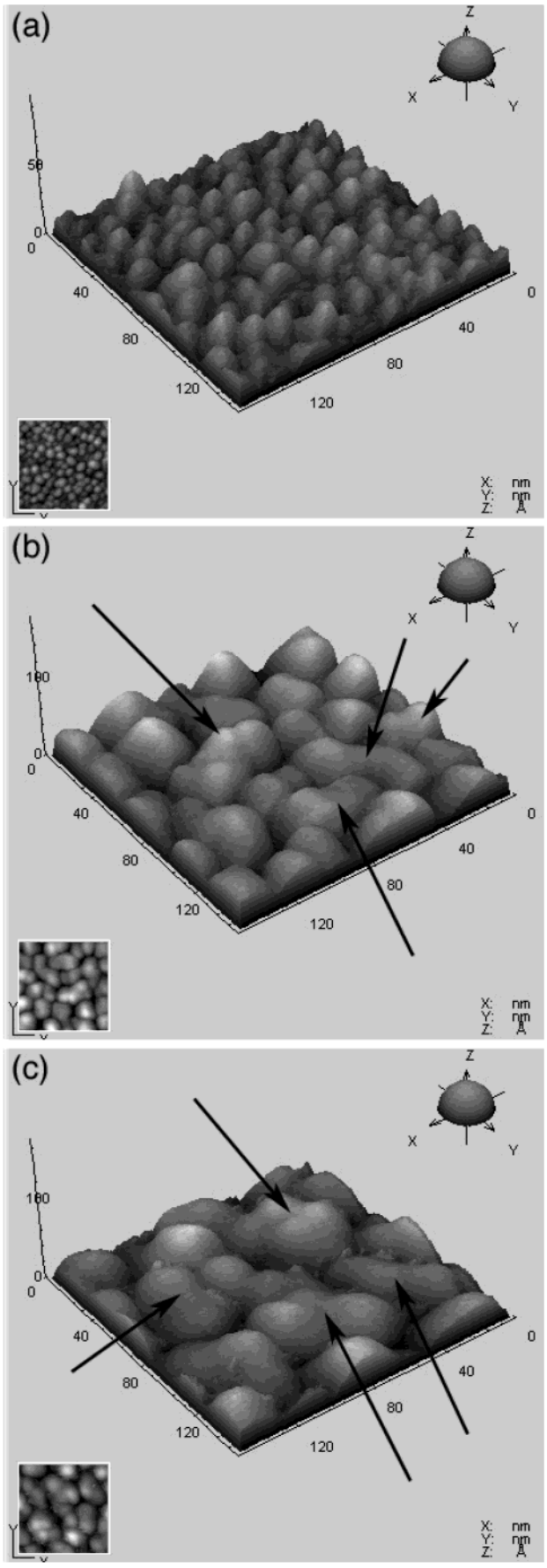

Figure 7. 3D AFM images (150 × 150 nm^2) of 2.5 nm (a), 5.0 nm (b), and 7.5 nm (c) unannealed Au island films. Arrows indicate coalescence of islands. *Z*-scale bar: 5 nm (a), 10 nm (b, c).

(45) Yu, X.; Duxbury, P. M.; Jeffers, G.; Dubson, M. A. *Phys. Rev. B* **1991**, *44*, 13163−13166.
(46) Norrman, S.; Andersson, T.; Granqvist, C. G.; Hunderi, O. *Phys. Rev. B* **1978**, *18*, 674−695.

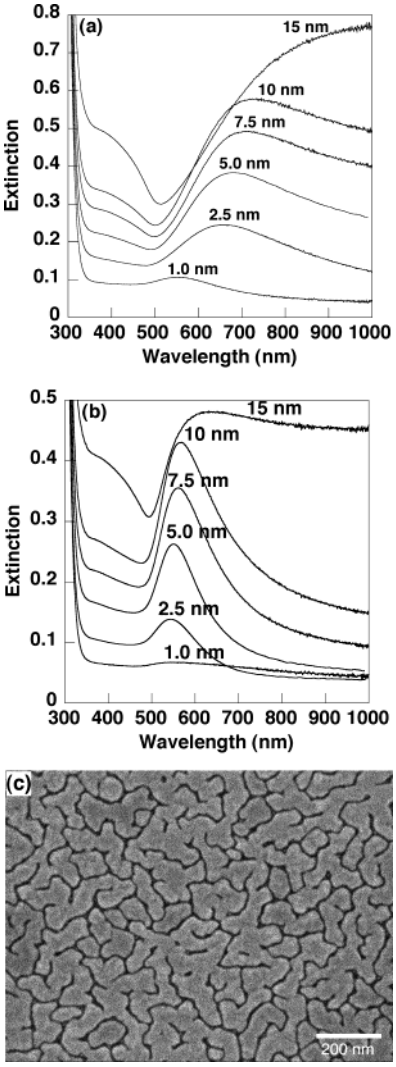

Figure 8. Transmission UV−vis spectra of ultrathin gold island films on silanized glass, (a) unannealed and (b) annealed 20 h at 200 °C. Nominal thicknesses are indicated. (c) HR-SEM image of a 15.0 nm unannealed Au film.

7b,c) with partial coalescence of smaller islands, promoting lower total island area and an increase in the average island height.[45] The percolation threshold is thus reached at a higher average coverage than that expected for simple growth without island mobility and coalescence (50% and 59% for triangular and square lattices, respectively[47]).

It should be noted that a more quantitative evaluation of the coalescence process is complicated by the induced temperature rise during the evaporation, influencing island mobility and aggregation.

Optical Properties of Au Island Films. Unannealed and annealed Au island films on silanized glass substrates were characterized by transmission UV−vis spectroscopy[2] after stabilization in a solvent (see Preparation and Stabilization of Au Island Films section). As was shown previously for Au island films on bare glass,[46] a red shift and an increase in the optical density are observed upon increasing the nominal thickness (Figure 8). The effect of annealing is seen in Figures 1 and 8; annealing induces a blue shift in the spectrum (up to 164 nm) and a decrease in the optical density (up to 0.15 au). The SP band is completely lost in the spectrum of the 15.0 nm unannealed Au film (Figure 8a), indicating a transition from island morphology to a continuous film.[46] This is in agreement with the HR-SEM imaging (Figures 8c), where a near-percolation situation, with micrometer-size connected Au areas, is observed for the 15.0 nm unannealed film. Careful inspection of the spectrum of the 1.0 nm annealed Au film reveals a longitudinal plasmon at longer wavelengths (700−800 nm) characteristic of chains of islands,[48,49] as was evident in the HR-SEM image of the corresponding film (Figure 2).

Conclusions

Evaporation of 1.0−15.0 nm (nominal thickness) gold at a slow rate (0.005−0.012 nm s^{-1}) on MPTS-treated glass substrates provides arrays of island-shaped Au films, stabilized by the MPTS adhesion layer. As was previously shown by us for Au island films on untreated transparent substrates, the films display an intense surface plasmon (SP) absorbance in the vis-to-NIR range, which is sensitive to the Au thickness, the evaporation conditions, postdeposition annealing, and exposure to solvents. Hence, immersion in 1:1 $CHCl_3$/EtOH solution led to a marked change in the SP absorbance, while no corresponding change in morphology could be seen by HR-SEM imaging, a point to be further investigated. As was shown previously,[2,23] increasing the Au nominal thickness promotes an increase in the intensity and a red shift of the Au SP band, whereas annealing leads to a decrease in the intensity and a blue shift of the SP band.

Analysis of HR-SEM and AFM images of the Au island films shows that the average island dimensions (lateral diameter and height) increase with nominal thickness. Annealing increases the average area of individual islands, the average island height, and the average separation between islands. Therefore, the fractional coverage of the glass by the Au is larger and increases faster for unannealed films. HR-SEM imaging and spectroscopic data both indicate a percolation transition around 15.0 nm (nominal thickness) for the unannealed (but not the annealed) films, exhibited as micrometer-scale conducting paths (HR-SEM imaging) and disappearance of the Au SP band (transmission spectroscopy). The combination of HR-SEM and AFM imaging proved to be rather powerful in providing a realistic view of the island shape.

Of the Au island films studied here, annealed films of 2.5−10.0 nm nominal thickness are relatively stable and display a well-defined SP band, thus being particularly promising for T-SPR spectroscopy and sensing applications.

Acknowledgment. We thank EU NANOPHOS project No. IST-2001-39112, and the Edward D. and Anna Mitchell Research Fund, Weizmann Institute, for financial support. A.V. is partially supported by a

(47) Stauffer, D.; Aharony, A. *Introduction to Percolation Theory*, 2nd ed.; Taylor & Francis: London, 1992.

(48) Liao, J. H.; Zhang, Y.; Yu, W.; Xu, L. N.; Ge, C. W.; Liu, J. H.; Gu, N. *Colloids Surf., A* **2003**, *223*, 177−183.

(49) Sawitowski, T.; Miquel, Y.; Heilmann, A.; Schmid, G. *Adv. Funct. Mater.* **2001**, *11*, 435−440.

KAMEA Fellowship, the Israel Ministry of Immigrant Absorption.

Supporting Information Available: Table of the experimental conditions of Au island film evaporation (PDF). This material is available free of charge via the Internet at http://pubs.acs.org.

CM049605A